

Т 64 (5)	ИЗВЕСТИЯ ВЫСШИХ УЧЕБНЫХ ЗАВЕДЕНИЙ. Серия «ХИМИЯ И ХИМИЧЕСКАЯ ТЕХНОЛОГИЯ»	2021
V 64 (5)	<b>ChemChemTech</b> IZVESTIYA VYSSHIKH UCHEBNYKH ZAVEDENII KHIMIYA KHIMICHESKAYA TEKHNOLOGIYA	2021

DOI: 10.6060/ivkkt.20216405.6060

УДК: 546.05:546.831:546.73

**СИНТЕЗ В СВЕРХКРИТИЧЕСКОМ ФЛЮИДЕ CO<sub>2</sub>  
НАНОРАЗМЕРНЫХ ДИОКСИДА ЦИРКОНИЯ, ОКСИДА КОБАЛЬТА И ФАЗ НА ИХ ОСНОВЕ**

**И.Е. Соколов, Р.М. Закалюкин, Е.В. Копылова, А.С. Кумсков,  
Р.Н. Можчиль, А.М. Ионов, В.В. Фомичев**

Илья Евгеньевич Соколов\*, Валерий Вячеславович Фомичев

Кафедра химии и технологии редких элементов им. К.А. Большакова, Институт тонких химических технологий им. М.В. Ломоносова, МИРЭА-Российский технологический университет, просп. Вернадского, 86, Москва, Российская Федерация, 119571

E-mail: sokolov\_iliya@yahoo.com\*, valeryfom@rambler.ru

Руслан Михайлович Закалюкин

Кафедра электротехнических систем, Институт радиотехнических и телекоммуникационных систем, МИРЭА-Российский технологический университет, просп. Вернадского, 78, Москва, Российская Федерация, 119454

Лаборатория процессов кристаллизации, Институт кристаллографии им. А.В. Шубникова, Ленинский просп., 59, Москва, Российская Федерация, 119333

E-mail: rmzakalyukin@mitht.ru

Елена Васильевна Копылова

Кафедра стандартизации и метрологии, Физико-технологический институт, МИРЭА-Российский технологический университет, просп. Вернадского, 78, Москва, Российская Федерация, 119454

E-mail: kopylova\_e@mirea.ru

Андрей Сергеевич Кумсков

Лаборатория электронной микроскопии, Институт кристаллографии им. А.В. Шубникова, Ленинский просп., 59, Москва, Российская Федерация, 119333

E-mail: a.kumskov@gmail.com

Раис Николаевич Можчиль

Кафедра физики твердого тела и наносистем, Институт лазерных и плазменных технологий, Национальный исследовательский ядерный университет «МИФИ», Каширское шоссе, 31, Москва, Российская Федерация, 115409

Лаборатория спектроскопии поверхности полупроводников, Институт физики твердого тела РАН, ул. Академика Осипяна, 2, Черноголовка, Московская обл., Российская Федерация, 142432

E-mail: mr\_mozhchil@mail.ru

Андрей Михайлович Ионов

Лаборатория спектроскопии поверхности полупроводников, Институт физики твердого тела РАН, ул. Академика Осипяна, 2, Черноголовка, Московская обл., Российская Федерация, 142432

E-mail: ionov@issp.ac.ru

*Данное исследование посвящено получению методом SAS в сверхкритическом диоксиде углерода наноразмерных диоксида циркония, оксида кобальта и фаз на их основе. Исходные растворы готовили путем добавления к ацетилацетонату циркония (IV) и ацетилацетонату кобальта (II) метилового спирта в заданных соотношениях, которые затем вносили в реактор. Параметры эксперимента при получении наночастиц имели следующие значения: давление 10 МПа, температура 50 °С, скорость подачи диоксида углерода 35 г/мин, скорость подачи исходного раствора 0,5 мл/мин. Были получены индивидуальные фазы, содержащие цирконий и кобальт, а также образцы с мольным соотношением циркония к кобальту: 3:1, 2:1, 1:1, 2:1, 1:3. Полученные образцы были охарактеризованы комплексом физико-химических методов анализа: инфракрасная спектроскопия, дифференциальная сканирующая калориметрия, рентгенофазовый анализ, просвечивающая электронная микроскопия, рентгеновская фотоэлектронная спектроскопия. Использование ацетилацетонатов циркония и кобальта в качестве исходных компонентов, приводит к образованию устойчивых продуктов – наночастиц ацетатов соответствующих металлов в рентгеноаморфном состоянии. При нагревании до 340-350 °С происходит разрушение металлоорганических комплексов до оксидов с образованием в системе  $ZrO_2 - CoO$  непрерывного ряда рентгеноаморфных твердых растворов. При температуре выше 600 °С происходит кристаллизация фаз с распадом твердых растворов на индивидуальные оксиды  $ZrO_2$  и  $Co_3O_4$ . При температуре выше 900 °С происходит дальнейшее окисление кобальта. Таким образом, процесс окисления оксида кобальта до  $Co_3O_4$  проходит в две стадии при 600 и 900 °С. Для образцов диоксида циркония с примесью оксида кобальта при температуре 700 °С наблюдается стабилизация кубической модификации, что вероятно, связано с входжением в кубическую структуру оксида циркония примеси кобальта, которая препятствует переходу в тетрагональную и моноклинную модификации.*

**Ключевые слова:** наночастицы, метод сверхкритического антисольвентного осаждения, оксид кобальта, диоксид циркония, просвечивающая электронная микроскопия

## SYNTHESIS OF NANOSIZED ZIRCONIUM DIOXIDE, COBALT OXIDE AND RELATED PHASES IN SUPERCRITICAL CO<sub>2</sub> FLUID

I.E. Sokolov, R.M. Zakalyukin, E.V. Kopylova, A.S. Kumskov,  
R.N. Mozhchil, A.M. Ionov, V.V. Fomichev

Ilya E. Sokolov\*, Valery V. Fomichev

Department of Chemistry and Technology of Rare Elements, Lomonosov Institute of Fine Chemical Technologies, MIREA – Russian Technological University, Vernadskogo ave., 86, Moscow, 119571, Russia  
E-mail: sokolov\_iliya@yahoo.com\*, valeryfom@rambler.ru

Ruslan M. Zakalyukin

Department of Electrotechnical Systems, The Institute of Radio Engineering and Telecommunication Systems, MIREA – Russian Technological University, Vernadskogo ave., 78, Moscow, 119454, Russia  
Laboratory of Crystallization Processes, Shubnikov Institute of Crystallography of Federal Scientific Research Centre “Crystallography and Photonics” of the RAS, Leninskiy ave., 59, Moscow, 119333, Russia  
E-mail: rmzakalyukin@mitht.ru

Elena V. Kopylova

Department of Standardization and Metrology, The Institute of Physics and Technology, MIREA – Russian Technological University, Vernadskogo ave., 78, Moscow, 119454, Russia  
E-mail: kopylova\_e@mirea.ru

Andrey S. Kumskov

Laboratory of Electron Microscopy, Shubnikov Institute of Crystallography of Federal Scientific Research Centre “Crystallography and Photonics” of the RAS, Leninskiy ave., 59, Moscow, 119333, Russia  
E-mail: a.kumskov@gmail.com

Rais N. Mozhchil

Department of Solid State Physics and Nanosystems, The Institute for Laser and Plasma Technologies, National Research Nuclear University MEPhI (Moscow Engineering Physics Institute), Kashirskoe Shosse, 31, Moscow, 115409, Russia

Laboratory of Semiconductor Surfaces Spectroscopy, The Institute of Solid State Physics of the RAS, Academician Ossipyan st., 2, Chernogolovka, Moscow District, 142432, Russia  
E-mail: mr\_mozhchil@mail.ru

Andrey M. Ionov

Laboratory of Semiconductor Surfaces Spectroscopy, The Institute of Solid State Physics of the RAS, Academician Ossipyan st., 2, Chernogolovka, Moscow District, 142432, Russia  
E-mail: ionov@issp.ac.ru

*This study is devoted to obtaining nanoscale zirconium dioxide, cobalt oxide and related phases by SAS method in supercritical carbon dioxide. The synthesized compounds were characterized by a complex of physico-chemical analytical methods: infrared spectroscopy, differential scanning calorimetry, X-ray diffraction, transmission electron microscopy, X-ray photoelectron spectroscopy. The experimental parameters for obtaining the nanoparticles were: pressure 10 MPa, temperature 40 °C, carbon dioxide supply rate 35 g/min, the initial solution supply rate 0.5 ml/min. Individual phases containing zirconium and cobalt, and also samples with zirconium to cobalt molar ratios 3:1, 2:1, 1:1, 2:1 and 1:3 were obtained. The use of zirconium and cobalt acetylacetonates as initial components leads to formation of stable products – nanoparticles of acetates of the corresponding metals in the X-ray amorphous state. When heated to 340-350 °C, the destruction of organometallic complexes to oxides occurs with formation of a continuous series of X-ray amorphous solid solutions in the ZrO<sub>2</sub>-CoO system. At temperatures above 600 °C, the phases crystallize with the decomposition of solid solutions into ZrO<sub>2</sub> and Co<sub>3</sub>O<sub>4</sub>. When temperature is above 900 °C, further oxidation of cobalt occurs. Thus, cobalt oxide oxidation into Co<sub>3</sub>O<sub>4</sub> proceeds in two steps, at 600 and 900 °C. For samples of zirconium dioxide with cobalt oxide admixture at a temperature of 700 °C stabilization of the cubic modification is observed which is probably due to the entry of cobalt into the cubic structure of zirconium oxide, which prevents transition to tetragonal and monoclinic modifications.*

**Key words:** nanoparticles, supercritical antisolvent precipitation technique, cobalt oxide, zirconium dioxide, transmission electron microscopy

**Для цитирования:**

Соколов И.Е., Закалюкин Р.М., Копылова Е.В., Кумсков А.С., Можчи́ль Р.Н., Ионо́в А.М., Фоми́чев В.В. Синтез в сверхкритическом флюиде CO<sub>2</sub> наноразмерных диоксида циркония, оксида кобальта и фаз на их основе. *Изв. вузов. Химия и хим. технология*. 2021. Т. 64. Вып. 5. С. 35–43

**For citation:**

Sokolov I.E., Zakalyukin R.M., Kopylova E.V., Kumskov A.S., Mozhchil R.N., Ionov A.M., Fomichev V.V. Synthesis of nanosized zirconium dioxide, cobalt oxide and related phases in supercritical CO<sub>2</sub> fluid. *ChemChemTech [Izv. Vyssh. Uchebn. Zaved. Khim. Khim. Tekhnol.]*. 2021. V. 64. N 5. P. 35–43

## INTRODUCTION

The nanosized zirconium dioxide becomes of greater and greater practical importance in many spheres of human life. Recently the use of ceramics in biomedicine has increased [1]. Zirconium dioxide is

applied also in a number of other medical branches, such as orthopedics and stomatology [2, 3]. Ceramics based on zirconium dioxide and aluminum oxide can be used as bone implants [4]. Special attention is paid to using zirconium dioxide as a catalyst or a catalyst carrier [5-7]. Zirconium dioxide modified by anions

such as sulfate ions forms a high-acidity or a superacid catalyst depending on the synthesis conditions [8, 9]. Such a catalyst has worked well in many important commercial processes, such as isomerization of hydrocarbons, alkylation, condensation, cyclization, Fischer-Tropsch reaction, cracking of oils and oil products and many others [10-15]. The surface characteristics of such catalysts can be improved by adding metal cations as promoters [16-18]. Using zirconium dioxide catalysts with addition of iron and cobalt oxides as active sites enables reducing nitrogen oxides [19, 20]. Complex oxide systems of cerium and yttrium stabilized by zirconium oxide were suggested as electrolytes for the solid-state fuel cells [21]. The development of low-temperature catalysts for carbon monoxide oxidation in the presence of hydrogen – cobalt, iron and copper oxides applied on zirconium dioxide – seems to be promising [22]. Utilization of carbon dioxide is equally important. This process utilizes cobalt- and iron-containing catalysts applied on zirconium dioxide or on aluminum gamma oxide [23, 24]. Zirconium oxide is used in sensors for detecting various gases (such as carbon monoxide, nitrogen oxides, ammonia, sulfur dioxide, hydrogen sulfide) in air [25, 26].

By now many methods for synthesizing zirconium dioxide and zirconium oxide based catalysts have been suggested: a sedimentation method, where nitrates of the corresponding metals are used as precursors [27, 28]; a sol-gel method and hydrothermal methods using zirconyl chloride or zirconium alcoholate as initial salts [29-32].

However, these methods have a number of shortcomings. Specifically, they do not make it possible to control particles morphology and prepare a product without impurities of the initial salts. From this point of view, the method of supercritical antisolvent precipitation (SAS) is promising. This method uses as precursors transition metal alcoholates dissolved in an organic solvent and supercritical CO<sub>2</sub> as an antisolvent. Using this method of synthesis allows to control finely the size and geometrical shape of particles by varying process parameters, such as pressure, temperature and the rate of solution or CO<sub>2</sub> delivery.

The authors published previously the results of studies on the synthesis of nanosized titanium and zirconium dioxides, as well as their solid solutions by supercritical antisolvent precipitation (SAS) with supercritical CO<sub>2</sub> [33-35]. The isopropylates of the corresponding metals in isopropanol were used as starting substances. The obtained nanoparticles had an X-ray amorphous structure, high specific surface area and porosity.

The goal of this work was to obtain and characterize nanosized zirconium dioxide, cobalt oxide and related phases using SAS in the supercritical fluid of CO<sub>2</sub>. Noteworthy, it is known that double oxides are not formed in the CoO – ZrO<sub>2</sub> system studied by the solid-phase synthesis methods.

## EXPERIMENTAL SECTION

### *Synthesis*

The nanosized samples of CoO – ZrO<sub>2</sub> system were synthesized in a SuperParticle SAS-50 System experimental unit ("Waters Corp"). The initial solutions were prepared by addition of methanol (HPLC, "LAB-SCAN") to zirconium (IV) acetylacetonate (98%, "Sigma-Aldrich") and to cobalt (II) acetylacetonate (97%, "Sigma-Aldrich") in preset ratios. Then the reaction mixtures were transferred into a reactor. After the experiment, CO<sub>2</sub> fluid was supplied for 15 min more to remove the solvent from the surface and from the volume of the obtained particles. The experimental parameters for obtaining the nanoparticles were: pressure 10 MPa, temperature 40 °C, CO<sub>2</sub> supply rate 35 g/min, the initial solution supply rate 0.5 ml/min. The individual phases containing zirconium and cobalt, and also samples with zirconium to cobalt molar ratios 3:1, 2:1, 1:1, 2:1 and 1:3 were obtained.

### *Research Methods*

The obtained samples were studied by a series of physicochemical methods. In order to remove traces of the organic solvent the samples were dried in an LT-VO/20 vacuum drying oven at 0.7 bar. The thermal analysis of the samples was carried out with the use of a synchronous SDT Q6000 TGA/DTA/DSC thermoanalyzer in ceramic crucibles. Curves were recorded in 10 °C/min increments up to 1000 °C in the air. The IR absorption spectra were registered with using Bruker EQUINOX55 Fourier spectrometer. Samples were prepared in the form of pellets with KBr. The X-ray studies were executed using Bruker D8 Advance diffractometer (Cu-K $\alpha$  radiation, a graphite monochromator). ICDD-JCPDS cards were used for the phase identification. A transmission electron FEI Osiris microscope equipped with a field emission source was used. Microphotographs were obtained at an accelerating voltage of 200 kV. Resolution: 0.12 nm in the light-field mode (TEM). The content of the organic component in the samples was controlled with the use of a ThermoQuest FLASH EA 1112 automatic C, H, N, S elemental analyzer.

The photoelectron studies were performed with KRATOS AXIS ULTRA DLD photoelectron spectrometer in ultra-high vacuum ( $5 \cdot 10^{-10}$  –  $3 \cdot 10^{-9}$  torr) using AlK $\alpha$  radiation at a photon energy of 1486.69 eV (energy resolution 0.48 eV, binding energy was calibrated using Ag3d<sub>5/2</sub> line).

## RESULTS AND DISCUSSION

Freshly prepared samples with various zirconium/cobalt ratios have amorphous structures, which were confirmed by a ring diffraction pattern obtained when studying by electron microscopy. The particles are agglomerates of 70-270 nm spherical bodies tightly bound with each other (Fig. 1).

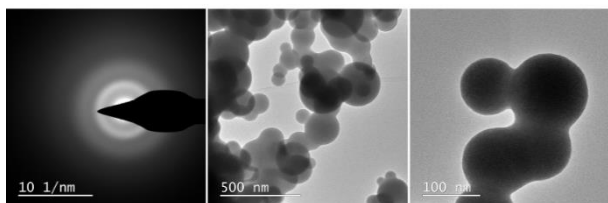


Fig. 1. Diffraction pattern and agglomerates of freshly prepared particles of sample with Co/Zr ratio 1:2

Рис 1. Дифракционная картина и агломераты свежеприготовленных частиц образца с соотношением Co/Zr 1:2

The registered IR absorption spectra show presence of acetate groups in freshly prepared samples. Absorption bands at 1585, 1381, 1025, 930 and 656  $\text{cm}^{-1}$  are attributed to these groups (Fig. 2) [36]. In addition, the qualitative reaction with iron chloride for confirmation the presence of acetate salts was carried out.

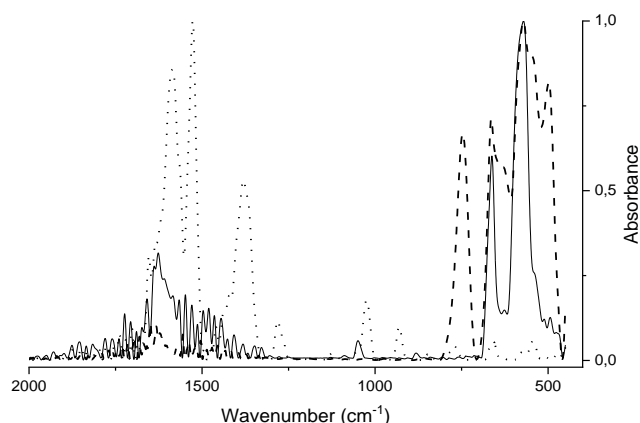


Fig. 2. The IR absorption spectrum of freshly prepared sample (dotted line) calcined at 700 °C (dashed line) and 1000 °C (solid line) with Co/Zr ratio 1:2

Рис. 2. ИК спектр поглощения свежеприготовленного образца (точечная линия), прокаленного при температуре 700 °C (пунктирная линия) и 1000 °C (сплошная линия) с соотношением Co/Zr 1:2

The mechanism of zirconium acetylacetonate thermal decomposition was studied by Ismail [37]. The authors found several intermediate products containing acetate groups:  $\text{Zr}(\text{C}_5\text{H}_7\text{O}_2)_2(\text{CH}_3\text{COO})_2$ ,  $\text{ZrOH}(\text{CH}_3\text{COO})_3$  and  $\text{ZrO}(\text{CH}_3\text{COO})_2$ .

Thermogravimetric analysis of a freshly prepared sample of zirconium acetate shows that heating to 340 °C results in a large weight loss (to 46.7%),

which is close to the theoretical value of 45.1% upon  $\text{ZrO}(\text{CH}_3\text{COO})_2$  zirconium acetate thermal decomposition to zirconium oxide  $\text{ZrO}_2$ . The synthesis specific features, can explain the excess of weight loss as compared to the theoretical value by the presence of a residual organic solvent (alcohol) in the large volume of the pore space according to early studies [33-35]. The C, H, N, S elemental analysis data presented in Table indicate that the excessive amounts of carbon and hydrogen are equal to 1.33% and 0.99%, respectively, with regard to the values theoretically calculated for zirconium acetate.

Table

**Results of the elemental analysis for freshly prepared zirconium acetate sample**

Таблица. Результаты анализа элементного состава свежеприготовленного образца ацетата циркония

Determined parameter	C % wt.	H % wt.
Theoretical value	21.33	2.67
Freshly prepared sample	22.66	3.66

Thus, it can be concluded that the synthesis from the supercritical  $\text{CO}_2$  fluid with the use of transition metal acetylacetonates as starting substances affords zirconium acetate  $\text{Zr}(\text{Ac})$  and cobalt acetate  $\text{Co}(\text{Ac})$  as the reaction products. They were transformed into oxides upon heating to 340 °C. The latter, according to the results of X-ray phase analysis, also have an amorphous structure.

Decomposition of individual zirconium acetate at 450 °C results in the nucleation of a cubic  $\text{ZrO}_2$  phase. The nucleation centers were identified by the existence of the most intensive peak (111) on the amorphous ring of the X-ray pattern.

Analysis of electronic microphotographs of analogous samples with various Co/Zr ratio shows uniform distribution of the chemical elements in the nanoparticles volume. This indicates the formation of a continuous series of solid solutions in the amorphous state of the  $\text{ZrO}_2 - \text{CoO}$  system (Fig. 3).

According to the results of thermogravimetric and X-ray phase analyses of the solid solution with Co/Zr ratio 1:2 two thermal effects with weight loss up to 5.30% were registered in the temperature range from 500 to 650 °C. They were attributed to the amorphous oxide crystallization and cobalt partial oxidation (Fig. 4). The latter was indicated by the emergence of a second component in the XPS spectrum. This is evidenced also by the X-ray phase analysis results. Most likely, in this case the weight loss is due to the residual solvent expelling from the pore space upon the substance crystallization.

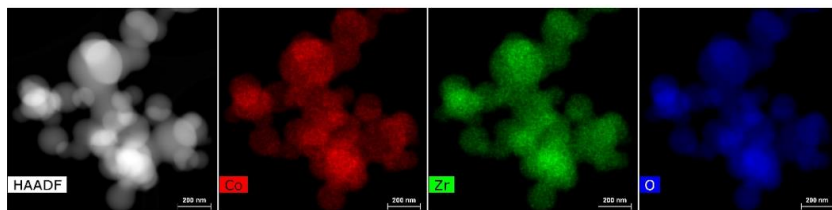


Fig. 3. The area of elemental analysis of a solid solution with Co/Zr ratio 1:2: a darkfield image and a distribution map for Co, Zr and O

Рис. 3. Область проведения элементного анализа твердого раствора с соотношением Co/Zr 1:2: темнопольное изображение и карта распределения элементов Co, Zr и O

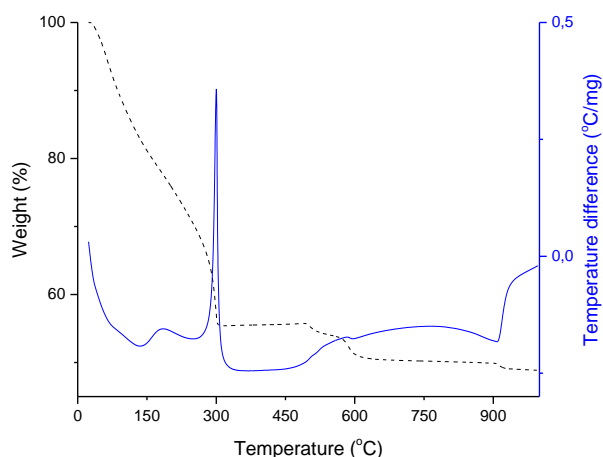


Fig. 4. TG/DSC (dashed/solid) curve of sample with Co/Zr ratio 1:2

Рис. 4. ТА/ДТА/ДСК образца с соотношением Co/Zr 1:2

Analysis of the electronic microphotographs of a sample with Co/Zr ratio 1:2 calcined at 700 °C (Co/Zr(Ac) 700 °C) shows nonuniform distribution of the chemical elements in the nanoparticles volume. This indicates the formation of  $\text{Co}_3\text{O}_4$  polycrystals on  $\text{ZrO}_2$  surface. Particles adhere to one another forming agglomerates. The particles size is from 70 to 260 nm. The high-resolution photograph clearly shows formation of the samples with crystalline structure (Fig. 5).

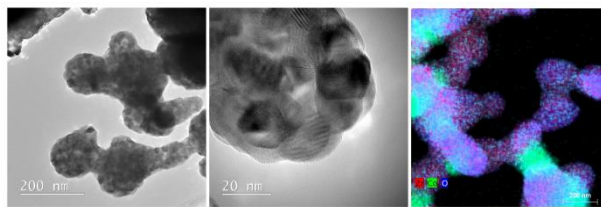


Fig. 5. Agglomerates of the particles of sample with Co/Zr ratio 1:2 calcined at 700 °C and a distribution map for Co, Zr and O  
Рис. 5. Агломераты частиц образца с соотношением Co/Zr 1:2, прокаленного при температуре 700 °C, и карта распределения элементов Co, Zr и O

The X-ray patterns of freshly prepared samples of zirconium and cobalt acetates, as well as their solid solutions calcined at various temperatures are shown in

Fig. 6. In case of individual zirconium and cobalt acetates, corresponding oxides  $\text{ZrO}_2$  and  $\text{Co}_3\text{O}_4$  were formed after calcination at 700 °C. The formation of the oxide crystal structures was also demonstrated by the emergence of characteristic intense bands at 661, 557 and 752  $\text{cm}^{-1}$  in the IR absorption spectra related to the vibrations of cobalt- and zirconium-oxygen polyhedra [38, 39]. The presence of an absorption band at 1625–1655  $\text{cm}^{-1}$  attributed to the water deformation vibration is probably due to the capture of water molecules by the pores of the samples under study and by potassium bromide (Fig. 2) [39].

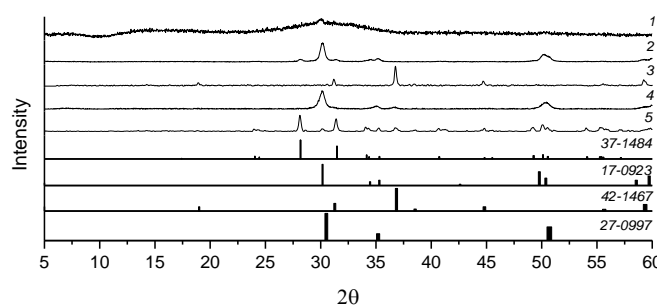


Fig. 6. The X-Ray patterns of freshly prepared samples calcined at different temperatures: Zr(Ac) 450 °C (1), Zr(Ac) 700 °C (2), Co(Ac) 700 °C (3), Co/Zr(Ac) 1:2 700 °C (4), Co/Zr(Ac) 1:2 1000 °C (5); ICDD–JCPDS: m- $\text{ZrO}_2$  (37-1484), t- $\text{ZrO}_2$  (17-0923), c- $\text{ZrO}_2$  (27-0997),  $\text{Co}_3\text{O}_4$  (42-1467)

Рис. 6. Рентгенограммы свежеприготовленных образцов, прокаленных при различных температурах: Zr(Ac) 450 °C (1), Zr(Ac) 700 °C (2), Co(Ac) 700 °C (3), Co/Zr(Ac) 1:2 700 °C (4), Co/Zr(Ac) 1:2 1000 °C (5); ICDD–JCPDS: m- $\text{ZrO}_2$  (37-1484), t- $\text{ZrO}_2$  (17-0923), c- $\text{ZrO}_2$  (27-0997),  $\text{Co}_3\text{O}_4$  (42-1467)

The X-ray pattern of a  $\text{ZrO}_2$  sample with cobalt oxide impurity Co/Zr 1:2 at 700 °C (Co/Zr(Ac) 700 °C) shows stabilization of the cubic modification (there is no multiplicity of the cubic phase peaks typical of X-ray patterns of the tetragonal and monoclinic phases). Most likely, it is due to the inclusion of a part of cobalt into zirconium oxide structure, which interferes with the cubic modification transformation into the tetragonal and monoclinic.

Heating up to 900 °C resulted in decomposition of the thermodynamically unstable cubic phase of zirconium oxide into the tetragonal and monoclinic phases. The transition to the monoclinic phase stable at this temperature is hindered. Therefore, it proceeds sequentially from the cubic phase via the tetragonal one, which was observed by the presence of the peaks of the monoclinic and tetragonal  $\text{ZrO}_2$  phases.

The last endothermic effect was registered at 909 °C. The X-ray pattern of a sample with Co/Zr ratio 1:2 calcined at 1000 °C (Co/Zr(Ac) 1000 °C) shows

both reflections of two polymorphic modifications of zirconium oxide and of cobalt (II, III) oxide. However, in this case the phase ratio is shifted towards the monoclinic modification of zirconium dioxide.

According to reference data cobalt (II) oxide is transformed into the mixed cobalt (II, III) oxide at a temperature over 500 °C and melts at a temperature over 977 °C [40]. As noted above, the X-ray pattern of a sample with Co/Zr ratio 1:2 calcined at 1000 °C shows presence of a signal of the mixed cobalt (II, III) oxide phase.

Nevertheless, according to the XPS data presented in Fig. 7, only one state  $\text{Co}^{2+}$  with Co 2p<sub>3/2</sub> binding energy 780 eV is present in the sample up to 450 °C. As calcination temperature increases to 700 °C, two states  $\text{Co}^{2+}$  and  $\text{Co}^{3+}$  with prevalence of the reduced cation (binding energy 780 and 780.3 eV, respectively) are present in the sample at the same time. When calcination temperature is 1000 °C, two states of cobalt are present as well. However, the ratio of oxidation degrees changes towards  $\text{Co}^{3+}$  with binding energy 780.3 eV.

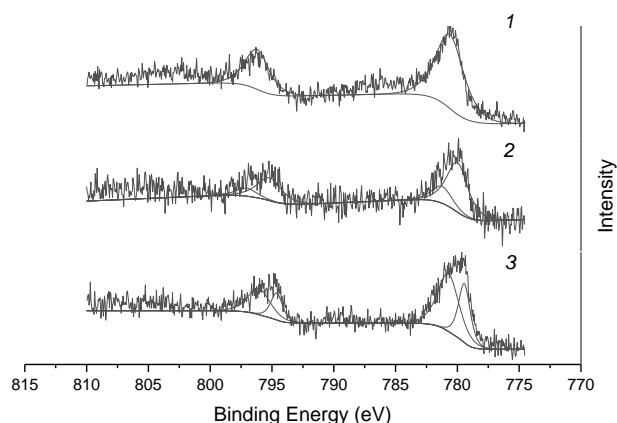


Fig. 7. The photoelectron spectrum of the Co2p region of the calcined samples with Co/Zr ratio 1:2: 450 °C (1), 700 °C (2), 1000 °C (3)  
Рис. 7. Фотоэлектронный спектр области Co2p образца с соотношением Co/Zr 1:2: 450 °C (1), 700 °C (2), 1000 °C (3)

### CONCLUSION

Synthesis in a  $\text{CO}_2$  supercritical fluid with the use of zirconium and cobalt acetylacetonates as initial components results in formation of stable products – nanoparticles of cobalt and zirconium acetates in an X-ray amorphous state. When heating to 340–350 °C, destruction of the organometallic complexes occurs to give the X-ray amorphous individual oxides or to form a continuous series of X-ray amorphous solid solutions in  $\text{ZrO}_2$  –  $\text{CoO}$  system. When temperature is increased above 600 °C, crystallization of phases with the solid solutions decomposition into individual zirconium and cobalt (II, III) oxides occurs. According to X-ray analysis results, it is possible to obtain pure cubic  $\text{ZrO}_2$  modification only for cobalt-containing samples.

When temperature is above 900 °C, further oxidation of cobalt occurs. Thus, cobalt oxide oxidation into  $\text{Co}_3\text{O}_4$  proceeds in two steps, at 600 and 900 °C.

### Conflicts of interest

There are no conflicts to declare.

### Acknowledgements

The work was carried out with the use of equipment of the Multiple-Access Center "Instrumental chemical analysis and complex research of substances and materials" of MIREA - Russian Technological University. The work was performed with the support of the Ministry of Science and Higher Education within the framework of the project of the Russian Fundamental Research Fund (project No. 18-29-06013). This work was supported by the Ministry of Science and Higher Education within the State assignment FSRC «Crystallography and Photonics» RAS in part of electron microscopy researches.

Работа выполнена с использованием оборудования Центра коллективного пользования «Инструментальный химический анализ и комплексное исследование веществ и материалов» МИРЭА-Российского технологического университета. Работа выполнена при поддержке Министерства науки и высшего образования в рамках выполнения работ по: Государственному заданию ФНИЦ «Кристаллография и фотоника» РАН; проекту Российского фонда фундаментальных исследований (проект № 18-29-06013).

### REFERENCES ЛИТЕРАТУРА

1. **Srinivas M., Buvanewari G.** A study of in vitro drug release from zirconia ceramics. *Trends Biomater Artif Organs*. 2006. V. 20. N 1. P. 24-30.
2. **Roualdes O., Duclos M.E., Gutknecht D., Frappart L., Chevalier J., Hartmann D.J.** In vitro and in vivo evaluation of an alumina–zirconia composite for arthroplasty applications. *Biomaterials*. 2010. V. 31. N 8. P. 2043-2054. DOI: 10.1016/j.biomaterials.2009.11.107.
3. **Oetzel C., Clasen R.** Preparation of zirconia dental crowns via electrophoretic deposition. *J. Mater. Sci*. 2006. V. 41. N 24. P. 8130-8137. DOI: 10.1007/s10853-006-0621-7
4. **He X., Zhang Y. Z., Mansell J. P., Su B.** Zirconia toughened alumina ceramic foams for potential bone graft applications: fabrication, bioactivation, and cellular responses. *J. Mater. Sci.: Materials in Medicine*. 2008. V. 19. N 7. P. 2743-2749. DOI: 10.1007/s10856-008-3401-x.
5. **Masudi A., Muraza O.** Zirconia-based nanocatalysts in heavy oil upgrading: a mini review. *Energy & fuels*. 2018. V. 32. N 3. P. 2840-2854. DOI: 10.1021/acs.energyfuels.7b03264.
6. **Park Y.M., Lee J.Y., Chung S.H., Park I.S., Lee S.Y., Kim D.K., Lee J.S., Lee K.Y.** Esterification of used vegetable oils using the heterogeneous  $\text{WO}_3/\text{ZrO}_2$  catalyst for production of biodiesel. *Biores. Technol*. 2010. V. 101. N 1. P. 59-61. DOI: 10.1016/j.biortech.2009.04.025.

7. Luo J., Xu H., Liu Y., Chu W., Jiang C., Zhao X. A facile approach for the preparation of biomorphic CuO–ZrO<sub>2</sub> catalyst for catalytic combustion of methane. *App. Catal. A: Gen.* 2012. V. 423. P. 121-129. DOI: 10.1016/j.apcata.2012.02.025.
8. Khan N.A., Mishra D.K., Ahmed I., Yoon J.W., Hwang J.S., Jung S.H. Liquid-phase dehydration of sorbitol to isosorbide using sulfated zirconia as a solid acid catalyst. *App. Catal. A: Gen.* 2013. V. 452. P. 34-38. DOI: 10.1016/j.apcata.2012.11.022.
9. Grecea M. L., Dimian A. C., Tanase S., Subbiah V., Rothenberg G. Sulfated zirconia as a robust superacid catalyst for multi-product fatty acid esterification. *Catal. Sci. Technol.* 2012. V. 2. N 7. P. 1500-1506. DOI: 10.1039/c2cy00432a.
10. Ejtemaei M., Aghdam N.C., Babaluo A.A., Tavakoli A., Bayati B. n-pentane isomerization over Pt-Al promoted sulfated zirconia nanocatalyst. *Sci. Iran. Transact. C, Chem., Chem. Eng.* 2017. V. 24. N 3. P. 1264-1271. DOI: 10.24200/sci.2017.4110.
11. Vlasov E.A., Myakin S.V., Sychov M.M., Aho A., Postnov A.Y., Mal'tseva N.V., Dolgashev A.O., Omarov Sh.O., Murzin D.Y. On Synthesis and Characterization of Sulfated Alumina–Zirconia Catalysts for Isobutene Alkylation. *Catal. Lett.* 2015. V. 145. N 9. P. 1651-1659. DOI: 10.1007/s10562-015-1575-7.
12. Yadav G. D., Ajgaonkar N. P., Varma A. Preparation of highly superacidic sulfated zirconia via combustion synthesis and its application in Pechmann condensation of resorcinol with ethyl acetoacetate. *J. Catal.* 2012. V. 292. P. 99-110. DOI: 10.1016/j.jcat.2012.05.004.
13. Marakatti V.S., Shanbhag G.V., Halgeri A.B. Sulfated zirconia; an efficient and reusable acid catalyst for the selective synthesis of 4-phenyl-1, 3-dioxane by Prins cyclization of styrene. *Appl. Catal. A: Gen.* 2013. V. 451. P. 71-78. DOI: 10.1016/j.apcata.2012.11.016.
14. Sousa-Aguiar E.F., Appel L.G. Catalysis involved in dimethylether production and as an intermediate in the generation of hydrocarbons via Fischer-Tropsch synthesis and MTG process. *Catalysis.* 2011. V. 23. P. 284-315. DOI: 10.1039/9781849732772-00284.
15. Permsubscul A., Vitidsant T., Damronglerd S. Catalytic cracking reaction of used lubricating oil to liquid fuels catalyzed by sulfated zirconia. *Korean J. Chem. Eng.* 2007. V. 24. N 1. P. 37-43. DOI: 10.1007/s11814-007-5006-3.
16. Gao S., Chen X., Wang H., Mo J., Wu Z., Liu Y., Weng X. Ceria supported on sulfated zirconia as a superacid catalyst for selective catalytic reduction of NO with NH<sub>3</sub>. *J. Colloid Interface Sci.* 2013. V. 394. P. 515-521. DOI: 10.1016/j.jcis.2012.12.034.
17. Zhang Y., Chen T., Zhang G., Wang G., Zhang H. Mesoporous Al-promoted sulfated zirconia as an efficient heterogeneous catalyst to synthesize isosorbide from sorbitol. *Appl. Catal. A: Gen.* 2018. V. 562. P. 258-266. DOI: 10.1016/j.apcata.2018.06.024.
18. Yang K., Li H., Zhao S., Lai S., Lai W., Lian Y., Fang W. Improvement of Activity and Stability of CuGa Promoted Sulfated Zirconia Catalyst for n-Butane Isomerization. *Indust. Eng. Chem. Res.* 2018. V. 57. N 11. P. 3855-3865. DOI: 10.1021/acs.iecr.7b04590.
19. Li N., Wang A., Zheng M., Wang X., Cheng R., Zhang T. Probing into the catalytic nature of Co/sulfated zirconia for selective reduction of NO with methane. *J. Catal.* 2004. V. 225. N 2. P. 307-315. DOI: 10.1023/a:1016667505736.
20. Zhang H., Li N., Li L., Wang A., Wang X., Zhang T. Selective Catalytic Reduction of NO with CH<sub>4</sub> Over In–Fe/Sulfated Zirconia Catalysts. *Catal. Lett.* 2011. V. 141. N 10. P. 1491-1497. DOI: 10.1039/c9ra06985b.
21. Chen K., Li N., Ai N., Li M., Cheng Y., Rickard W.D., Jiang S.P. Direct application of cobaltite-based perovskite cathodes on the yttria-stabilized zirconia electrolyte for intermediate temperature solid oxide fuel cells. *J. Mater. Chem. A.* 2016. V. 4. N 45. P. 17678-17685. DOI: 10.1039/c6ta07067a.
22. Firsova A.A., Khomenko T.I., Sil'chenkova O.N., Korchak V.N. Oxidation of carbon monoxide in the presence of hydrogen on the CuO, CoO, and Fe<sub>2</sub>O<sub>3</sub> oxides supported on ZrO<sub>2</sub>. *Kinet. Catal.* 2010. V. 51. N 2. P. 299-311. DOI: 10.1134/s0023158410020205.
23. Özkara-Aydınoglu Ş., Aksoylu A.E. Carbon dioxide reforming of methane over Co-X/ZrO<sub>2</sub> catalysts (X= La, Ce, Mn, Mg, K). *Catal. Commun.* 2010. V. 11. N 15. P. 1165-1170. DOI: 10.1016/j.catcom.2010.07.001.
24. Firsova A.A., Tyulenin Y.P., Khomenko T.I., Korchak V.N., Krylov O.V. Methane reforming with carbon dioxide on cobalt-containing catalysts. *Kinet. Catal.* 2003. V. 44. N 6. P. 819-826. DOI: 10.1023/b:kica.0000009060.12818.29.
25. Liu T., Zhang X., Yuan L., Yu J. A review of high-temperature electrochemical sensors based on stabilized zirconia. *Solid State Ionics.* 2015. V. 283. P. 91-102. DOI: 10.1016/j.ssi.2015.10.012.
26. Miura N., Sato T., Anggraini, S. A., Ikeda H., Zhuiykov S. A review of mixed-potential type zirconia-based gas sensors. *Ionics.* 2014. V. 20. N 7. P. 901-925. DOI: 10.1007/s11581-014-1140-1.
27. Arena F., Barbera K., Italiano G., Bonura G., Spadaro L., Frusteri F. Synthesis, characterization and activity pattern of Cu–ZnO/ZrO<sub>2</sub> catalysts in the hydrogenation of carbon dioxide to methanol. *J. Catalysis.* 2007. V. 249. N 2. P. 185-194. DOI: 10.1016/j.jcat.2007.04.003.
28. Tada S., Watanabe F., Kiyota K., Shimoda N., Hayashi R., Takahashi M., Nariyuki A., Igarashi A., Satokawa S. Ag addition to CuO-ZrO<sub>2</sub> catalysts promotes methanol synthesis via CO<sub>2</sub> hydrogenation. *J. Catalysis.* 2017. V. 351. P. 107-118. DOI: 10.1021/acscatal.6b01805.
29. Shao G.N., Imran S.M., Jeon S.J., Engole M., Abbas N., Haider M.S., Kang S.J., Kim H.T. Sol–gel synthesis of photoactive zirconia–titania from metal salts and investigation of their photocatalytic properties in the photodegradation of methylene blue. *Powder Technol.* 2014. V. 258. P. 99-109. DOI: 10.1016/j.powtec.2014.03.024.
30. Zhang P., Choy K.L. The Synthesis of Single Tetragonal Phase Zirconia by Sol-Gel Route. *Int. J. Eng. Res. & Sci.* 2015. P. 20-21.
31. Wang P., Zhao Z.D., Chen S.X., Fan G.R. Hydrothermal Synthesis of Mesoporous Nanocrystalline Tetragonal ZrO<sub>2</sub> Using Dehydroabietyltrimethyl Ammonium Bromine. *BioResources.* 2015. V. 10. N 1. P. 1271-1284. DOI: 10.15376/biores.10.1.1271-1284.



32. **Tomar L.J., Bhatt P.J., Desai R.K., Chakrabarty B.S.** Enhancement of optical properties of hydrothermally synthesized TiO<sub>2</sub>/ZrO<sub>2</sub> nanoparticles by Al, Ce Co-doping. *AIP Publishing*. 2015. V. 1665. N 1. P. 050124. DOI: 10.1063/1.4917765.
33. **Kononov I.A., Mavrin B.N., Prokudina N.A., Fomichev V.V.** Synthesis of nanoscale titanium dioxide by precipitation using supercritical anti-solvent. *Russ. Chem. Bull.* 2016. V. 65. N 12. P. 2795-2800. DOI: 10.1007/s11172-016-1658-7.
34. **Sokolov I.E., Kononov I.A., Zakalyukin R.M., Golubev D.V., Kumskov A.S., Fomichev V.V.** Synthesis of nanosized zirconium dioxide and its solid solutions with titanium dioxide from the CO<sub>2</sub> supercritical fluid. *MRS Commun.* 2018. V. 8. N 1. P. 59-64. DOI: 10.1557/mrc.2018.3.
35. **Смирнова К.А., Фомичев В.В., Дробот Д.В., Никишина Е.Е.** Получение наноразмерных пентаоксидов ниобия и тантала методом сверхкритического флюидного анти-сольвентного осаждения. *Тонкие химические технологии*. 2015. Т. 10. № 1. С. 76-82. **Smirnova K.A., Fomichev V.V., Drobot D.V., Nikishina E.E.** Obtaining nanosized pentoxides of niobium and tantalum by supercritical fluid antisolvent precipitation. *Fine Chem.Technol.* 2015. V. 10. N. 1. P. 76-82 (in Russian).
36. **Ito K., Bernstein H.J.** The vibrational spectra of the formate, acetate, and oxalate ions. *Canad. J. Chem.* 1956. V. 34. N 2. P. 170-178. DOI: 10.1139/v56-021.
37. **Ismail H.M.** Characterization of the decomposition products of zirconium acetylacetonate: nitrogen adsorption and spectrothermal investigation. *Powder Technol.* 1995. V. 85. N 3. P. 253-259. DOI: 10.1016/0032-5910(95)03025-7.
38. **López E.F., Escribano V.S., Panizza M., Carnasciali M.M.** Vibrational and electronic spectroscopic properties of zirconia powders. *J. Mater. Chem.* 2001. V. 11. N 7. P. 1891-1897. DOI: 10.1039/b100909p.
39. **Guan H., Shao C., Wen S., Chen B., Gong J., Yang X.** A novel method for preparing Co<sub>3</sub>O<sub>4</sub> nanofibers by using electrospun PVA/cobalt acetate composite fibers as precursor. *Mater. Chem. Phys.* 2003. V. 82. N 3. P. 1002-1006. DOI: 10.1016/j.matchemphys.2003.09.003.
40. **Kale G.M., Pandit S.S., Jacob K.T.** Thermodynamics of cobalt (II, III) oxide (Co<sub>3</sub>O<sub>4</sub>): Evidence of phase transition. *Transact. Jap. Inst. Metals.* V. 29. N 2. P. 125-132. DOI: 10.2320/matertrans1960.29.125.

Поступила в редакцию 16.05.2019  
Принята к опубликованию 05.04.2021

Received 16.05.2019  
Accepted 05.04.2021